Chemistry–A European Journal
Research Article
doi.org/10.1002/chem.202203634
Chemistry Europe
European Chemical Societies Publishing
www.chemeurj.org

Gold Teflates Revisited: From the Lewis Superacid $[Au(OTeF_5)_3]$ to the Anion $[Au(OTeF_5)_4]^-$

Marlon Winter,[a] Natallia Peshkur,[a] Mathias A. Ellwanger,[a, b] Alberto Pérez-Bitrián,[a] Patrick Voßnacker,[a] Simon Steinhauer,[a] and Sebastian Riedel*[a]

Abstract: A new synthetic access to the Lewis acid $[Au(OTeF_5)_3]$ and the preparation of the related, unprecedented anion $[Au(OTeF_5)_4]^-$ with inorganic or organic cations starting from commercially available and easy-to-handle gold chlorides are presented. In this first extensive study of the Lewis acidity of a transition-metal teflate complex by using different experimental and quantum chemical methods, $[Au(OTeF_5)_3]$ was classified as a Lewis superacid. The solid-state structure of the triphenylphosphine oxide adduct $[Au(OPPh_3)(OTeF_5)_3]$ was determined, representing the first structural characterization of an adduct of this highly reactive $[Au(OTeF_5)_3]$. Therein, the coordination environment around the gold center slightly deviates from the typical square planar geometry. The $[Au(OTeF_5)_4]^-$ anion shows a similar coordination motif.

Introduction

Since the definition by *Lewis* in 1923 that acids and bases are electron pair acceptors and donors, respectively,[1] the study of Lewis acids and their reactivity has led to various applications in organic synthesis, mainly as catalysts in different functionalization reactions.[2] Apart from the classical metal fluorides like SbF_5, which is the strongest conventional, binary Lewis acid, recent studies have focused on the preparation of strong Lewis acids containing bulkier O-, N- or C-donor ligands, mainly with main group elements, for example $[Al(OC(CF_3)_3)_3]$,[3] $[Al(N(C_6F_5)_2)_3]$[4] and $[B(p\text{-}CF_3\text{–}C_6F_4)_3]$.[5] In addition to their easier handling, some of these novel Lewis acids even exceed the fluoride ion affinity (FIA) of SbF_5 and can therefore be classified as Lewis superacids.[3,6]

In this regard, the pentafluoroorthotellurate (–$OTeF_5$, teflate) group has been known to combine strong electron-withdrawing properties and high charge capacity with an increased steric demand, therefore being able to stabilize elements in high oxidation states and reactive species,[7,8] for example $[As(OTeF_5)_5]$,[9,10] $Xe(OTeF_5)_2$,[11] or $[U(OTeF_5)_6]$.[12] Recently, $[Al(OTeF_5)_3]$ was prepared[13] and classified as a Lewis superacid[14] and the corresponding Brønsted acid was used to successfully protonate white phosphorus.[15] Furthermore, the first homoleptic nickel teflate complex $[Ni(OTeF_5)_4]^{2-}$ was prepared including a study of the properties of the teflate ligand in coordination chemistry.[16]

The gold teflate $[Au(OTeF_5)_3]$ was first prepared and characterized as a dimer (see below) by *Seppelt* and co-workers in 1985 but no further reactivity was investigated so far.[17] This compound can therefore be seen as the teflate analogue of AuF_3, which is a polymer in the solid state[18] and due to the relatively low Au–F bond energy compared to other E–F bonds (E=B, C, Si, P, among others),[19] it reacts violently with organic material.[20] Recent investigations show that the substitution of a fluorido ligand by a teflate in a gold(III) complex leads to an increase in Lewis acidity.[21] Therefore, we envisioned that $[Au(OTeF_5)_3]$ should combine a higher Lewis acidity with an increased stability due to the absence of reactive Au–F bonds.

Herein, we report on a new synthetic route to $[Au(OTeF_5)_3]$ and an extensive study of its Lewis acidity, which is, to our knowledge, the first experimental investigation of the Lewis acidity of a transition-metal teflate complex. Furthermore, we present the preparation of the hitherto unknown $[Au(OTeF_5)_4]^-$ anion with both inorganic and organic cations, which surprisingly has not been reported before, even though the complex anion can often be easier obtained than the corresponding Lewis acid.

[a] *M. Winter, N. Peshkur, Dr. M. A. Ellwanger, Dr. A. Pérez-Bitrián, P. Voßnacker, Dr. S. Steinhauer, Prof. Dr. S. Riedel*
Fachbereich Biologie, Chemie, Pharmazie
Institut für Chemie und Biochemie – Anorganische Chemie
Freie Universität Berlin
Fabeckstr. 34/36, 14195 Berlin (Germany)
E-mail: s.riedel@fu-berlin.de

[b] *Dr. M. A. Ellwanger*
Inorganic Chemistry Laboratory
Department of Chemistry
University of Oxford
South Parks Road, Oxford, OX1 3QR (UK)

Supporting information for this article is available on the WWW under https://doi.org/10.1002/chem.202203634

Results and Discussion

The Lewis Acid Tris(pentafluoroorthotellurato)gold(III)

We developed a new synthetic route for the preparation of $[Au(OTeF_5)_3]$, starting from the more easy-to-handle and available $AuCl_3$ and an excess of $ClOTeF_5$[22,23] as the teflate-transfer reagent, which has had only limited use for the introduction of teflate groups as of now[9,16,24] – in contrast to the literature-known procedure using AuF_3 and $[B(OTeF_5)_3]$.[17] Since $ClOTeF_5$ is a liquid at standard conditions, the reaction can be performed in neat $ClOTeF_5$ at room temperature (Scheme 1). The formation of chlorine during the reaction was confirmed by recording a UV/Vis spectrum of the gas phase (cf. Figure S24). We did not succeed in growing crystals suitable for single crystal X-ray diffraction by sublimation as it was shown in the literature.[17] However, the purity of the orange product was confirmed by powder X-ray diffraction (cf. Figure S3). Note, that $[Au(OTeF_5)_3]$ has a dimeric structure in the solid state with two bridging and four terminal $OTeF_5$ ligands, resulting in a near square planar coordination of the gold(III) centers (cf. Scheme 1 and Figure 1).

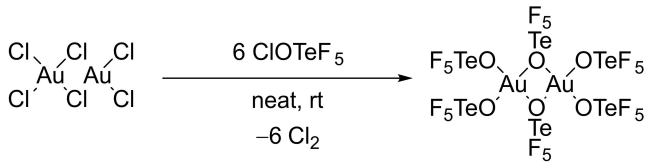

Scheme 1. Synthetic route to the dimeric Lewis acid $[Au_2(OTeF_5)_6]$ using Au_2Cl_6 and an excess of $ClOTeF_5$.

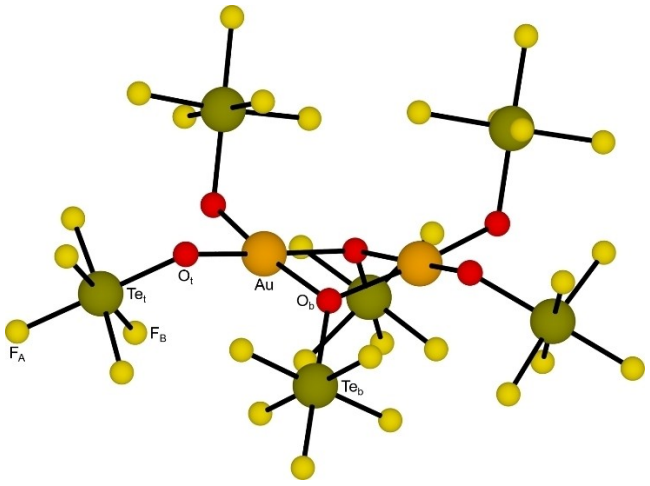

Figure 1. Optimized minimum structure of $[Au_2(OTeF_5)_6]$ on the RI-B3LYP-D3/def2-TZVPP level of theory. Average bond lengths [pm] with the range in brackets: 195.5(2) (Au–O_t), 208.7(6) (Au–O_b), 190.5(2) (O_t–Te), 194.6(8) (O_b–Te), 184.9(2) (Te_t–F_A), 184.0(1) (Te_b–F_A), 186(2) (Te_t–F_B), 185(1) (Te_b–F_B). Average bond angles [°] with the range in brackets: 92.0(7) (O_t–Au–O_t), 94.4(9) (O_t–Au–O_b, *cis*), 172.4(6) (O_t–Au–O_b, *trans*), 79.0(2) (O_b–Au–O_b), 97.5(3) (Au–O_b–Au), 122(3) (Au–O_t–Te_t), 125(3) (Au–O_b–Te_b), 178.2(7) (O_t–Te_t–F_A), 178.5(4) (O_b–Te_b–F_A), 91(4) (O_t–Te_t–F_B), 90(2) (O_b–Te_b–F_B), 89(2) (F_A–Te_t–F_B), 90.3(7) (F_A–Te_b–F_B), 89.8(9) (F_B–Te_t–F_B, *cis*), 177(2) (F_B–Te_t–F_B, *trans*), 90.0(1) (F_B–Te_b–F_B, *cis*), 179.0(2) (F_B–Te_t–F_B, *trans*). Note that the subscripts b and t denote O and Te atoms that are bridging and terminal, respectively, while A and B specify F atoms that are *trans* or *cis*, respectively, to the corresponding O atom of the –$OTeF_5$ group.

The Raman spectrum contains all bands reported in the literature,[17] but also additional minor bands at 754, 732, 725, 715, 652 and 637 cm^{-1}, which are in the typical region of Te–F stretching vibrations, and 326 cm^{-1}, which is in the region of Te–F deformation vibrations.[13] Both the experimental Raman and IR spectrum (the latter including the FIR region, cf. Figure S20) show a good agreement with the calculated spectra of the dimer at the RI-B3LYP-D3/def2-TZVPP level of theory (cf. Figure 1).

In order to investigate the Lewis acidity of $[Au(OTeF_5)_3]$ thoroughly, we performed the Gutmann-Beckett test,[25,26] recorded the frequency of the CN stretching vibration for the acetonitrile adduct,[27–29] and calculated the reaction enthalpies for the adduct formation of some Lewis bases including the fluoride ion affinity (FIA).[30,31]

In the Gutmann-Beckett method, the variation of the chemical shift of Et_3PO in the $^{31}P\{^1H\}$ NMR spectrum upon formation of an adduct with the Lewis acid of interest is investigated.[25,26] The stronger the shift $\Delta\delta(^{31}P)$ with regard to uncoordinated Et_3PO, the higher the acceptor number AN (AN = 2.21 ($\delta(^{31}P)-41$))[25] and thus, the higher the Lewis acidity. For $[Au(OPEt_3)(OTeF_5)_3]$, a chemical shift of $\delta(^{31}P) = 106.1$ ppm is observed in the $^{31}P\{^1H\}$ NMR spectrum (cf. Figure S6), which is shifted by $\Delta\delta(^{31}P) = 55.9$ ppm with respect to free Et_3PO ($\delta(^{31}P) = 50.2$ ppm) and corresponds to AN = 143.8. This AN is much higher than that of $[Au(CF_3)_3]$ (AN = 85.3).[32] Note that in the case of Et_3PO, the reaction needs to be done at −40 °C, since at room temperature further species are formed. Therefore, Ph_3PO was used as a similar but bulkier ligand, for which also Lewis acidity trends are known.[33,34] For $[Au(OPPh_3)(OTeF_5)_3]$, there is only one signal in the $^{31}P\{^1H\}$ NMR spectrum (cf. Figure S9) at room temperature at $\delta(^{31}P) =$ 66.5 ppm, being shifted by $\Delta\delta(^{31}P) = 37.2$ ppm with respect to free Ph_3PO ($\delta(^{31}P) = 29.3$ ppm).[33] This shift is significantly larger than in $[Au(CF_3)_3]$ ($\Delta\delta(^{31}P) = 20.6$ ppm).[32]

Cooling a concentrated solution of $[Au(OPPh_3)(OTeF_5)_3]$ in DCM to −24 °C yielded single crystals suitable for X-ray diffraction. $[Au(OPPh_3)(OTeF_5)_3]$ crystallizes in the monoclinic space group $P2_1/n$ and is the first solid-state structure of an $[Au(OTeF_5)_3]$ adduct. Interestingly, the coordination around the gold(III) center is slightly distorted from the typical square planar geometry (cf Figure 2). While the angles α(O–Au–O) involving two oxygen atoms in *cis* position to each other are close to the expected 90° (88.8(2)°–91.3(2)°), α(O–Au–O) with *trans*-oriented oxygen atoms are lower than 180° (172.8(2)° and 173.0(2)°). Using the four-coordinate geometry index τ_4 ($\tau_4 = (360°-(\alpha+\beta))/141°$; α and β are the two largest angles) implemented by *Houser* et al.,[35] $\tau_4 = 0.10$ was determined, which is still close to the ideal square planar geometry ($\tau_4 = 0$). Due to the fact that the ligands are alternately oriented above and below the distorted square planar $\{AuO_4\}$ unit, the distance between the ligands is maximized, yielding a closest distance between two fluorine atoms of adjacent teflate groups of 301.4(6) pm. However, this structural motif is also a local minimum structure in quantum chemical calculations on the RI-

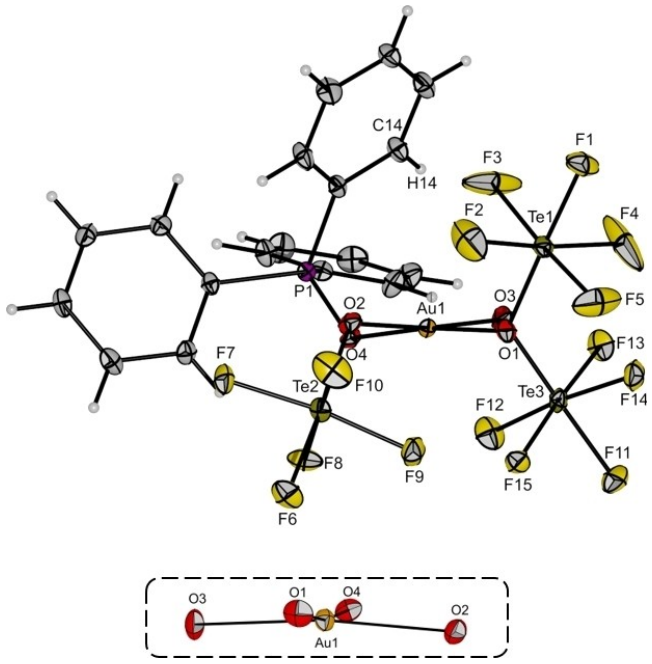

Figure 2. Molecular structure of $[Au(OPPh_3)(OTeF_5)_3]$ in the solid state (top) and excerpt of the $\{AuO_4\}$ unit highlighting the deviation from a square planar coordination (bottom). Thermal ellipsoids are set at 50% probability. Bond lengths [pm] and angles [°] involving the gold atom: 197.3(3) (Au1–O1), 197.7(3) (Au1–O2), 197.3(3) (Au1–O3), 197.3(3) (Au1–O4); 91.3(2) (O1–Au1–O2), 90.2(2) (O1–Au1–O3), 172.8(2) (O1–Au1–O4), 173.0(2) (O2–Au1–O3), 90.6(2) (O2–Au1–O4), 88.8(2) (O3–Au1–O4). The closest F–F distance of two adjacent $-OTeF_5$ groups is 301.4(6) pm (F4–F14).

B3LYP-D3/def2-TZVPP level (see Figure S26) and about 3 kJ mol^{-1} lower in energy than a structure similar to the $[I(OTeF_5)_4]^-$ anion[36] (see below), which is a transition state.

The Au–O bond lengths in $[Au(OPPh_3)(OTeF_5)_3]$ are between 197.3(3) pm and 197.7(3) pm. Compared to the Lewis acid itself, which is a dimer in the solid state, the bond lengths are significantly longer than those to the terminal oxygen atoms ($r(Au–O_{terminal}) = 178(4)$ pm and 182(3) pm) and significantly shorter than those to the bridging oxygen atoms ($r(Au–O_{bridging}) = 223(4)$ pm and 229(4) pm).[17] The only other known neutral, monomeric gold teflate species characterized by X-ray diffraction is $[AuF_2(OTeF_5)(SIMes)]$ with an Au–O bond length of 205.7(4) pm,[21] which is about 8 pm longer than in $[Au(OPPh_3)(OTeF_5)_3]$, due to the strong *trans*-influence of the *N*-heterocyclic carbene ligand. However, the *trans*-influence of the $-OPPh_3$ ligand seems to be similar to that of the $-OTeF_5$ group, since all Au–O bond lengths do not deviate significantly.

The acetonitrile adduct of $[Au(OTeF_5)_3]$ was prepared in order to investigate the blue shift in the stretching vibration ν(C≡N) compared to uncoordinated acetonitrile. A strong blue shift of ν(C≡N) in the IR spectrum is attributed to a strong Lewis acidity. Since for complexes with CH_3CN there is a Fermi resonance between ν(C≡N) and the combination mode (ν(C–C) + $\delta(CH_3)$), CD_3CN can be used for the adduct formation to circumvent this problem and get a more accurate value for the shift.[27–29] Therefore, the complex $[Au(CD_3CN)(OTeF_5)_3]$ was prepared by the addition of a stoichiometric amount of CD_3CN into a suspension of $[Au(OTeF_5)_3]$ in DCM. The IR spectrum of $[Au(CD_3CN)(OTeF_5)_3]$ (cf. Figure S21) shows a band at 2335 cm^{-1}, which is shifted by 73 cm^{-1} with respect to free CD_3CN (2262 cm^{-1}).[37] This shift is identical to the $SbF_5{\cdot}CD_3CN$ adduct.[27]

The ^{19}F NMR spectrum of a solution of $[Au(CD_3CN)(OTeF_5)_3]$ in CD_2Cl_2 consists of two AB_4X patterns, typical for $-OTeF_5$ groups, in a ratio of 2:1, as expected for the chemically inequivalent teflate ligands *cis* and *trans* to the CD_3CN ligand, highlighted in orange and red in Figure 3, respectively. The spectrum was successfully simulated so as to determine the parameters of interest (see Figure 3). Herein, the $-OTeF_5$ groups in *cis* position have a chemical shift of $\delta(F_{A,c}) = -44.5$ ppm and $\delta(F_{B,c}) = -49.1$ ppm with a coupling constant of $^2J(^{19}F_{A,c}, ^{19}F_{B,c}) =$ 181 Hz. For the teflate ligand in *trans* position to CD_3CN, the following values are obtained: $\delta(F_{A,t}) = -43.5$ ppm, $\delta(F_{B,t}) = -49.3$ ppm and $^2J(^{19}F_{A,t}, ^{19}F_{B,t}) = 182$ Hz. All values are in the typical range for compounds containing covalently bound $-OTeF_5$ groups.

In the ^{125}Te NMR spectrum, the chemical shifts of the tellurium atoms can be found at 586 ppm and 587 ppm for the teflate ligands in *cis* and *trans* position to CD_3CN, respectively. However, the pattern is of higher order and cannot be properly simulated only considering the parameters obtained by the simulation of the AB_4X pattern in the ^{19}F NMR spectrum. Furthermore, a long-range coupling of the tellurium atom in *cis* position with the F_B fluorine atoms of the $-OTeF_5$ ligand in *trans* position and vice versa needs to be included (see Figure 4 and Figure S10). The values are $^5J(^{125}Te_c, ^{19}F_{B,t}) = 31$ Hz and $^5J(^{125}Te_t, ^{19}F_{B,c}) = 32$ Hz for the tellurium atoms in *cis* and *trans* position, respectively.

In order to further estimate and compare the Lewis acidity of $[Au(OTeF_5)_3]$, quantum chemical calculations of the FIA were done by performing isodesmic reactions with the trimethylsilyl fluoride anchor point on the RI-BP86/def-SV(P) level.[30,31]

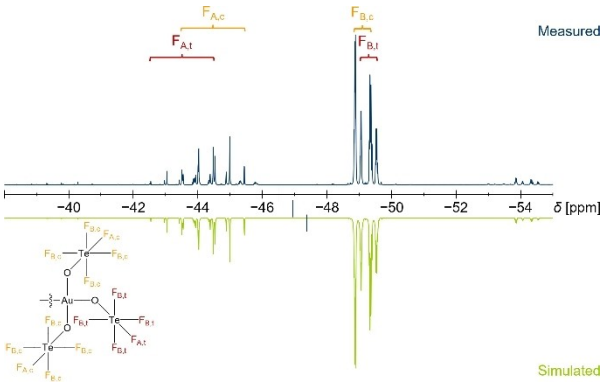

Figure 3. ^{19}F NMR spectrum (377 MHz, DCM-d_2, 20 °C) of $[Au(CD_3CN)(OTeF_5)_3]$ (top, blue) compared to the simulated spectrum (bottom, green). NMR spectroscopical parameters used in the simulation for the two $-OTeF_5$ ligands in *cis* position to CD_3CN: $\delta(F_{A,c}) = -44.5$ ppm, $\delta(F_{B,c}) = -49.1$ ppm, $^2J(^{19}F_{A,c}, ^{19}F_{B,c}) = 181$ Hz, $^1J(^{19}F_{A,c}, ^{125}Te_c) = 3535$ Hz, $^1J(^{19}F_{B,c}, ^{125}Te_c) = 3751$ Hz. NMR spectroscopical parameters used in the simulation for the $-OTeF_5$ ligand in *trans* position to CD_3CN: $\delta(F_{A,t}) = -43.5$ ppm, $\delta(F_{B,t}) = -49.3$ ppm, $^2J(^{19}F_{A,t}, ^{19}F_{B,t}) = 182$ Hz, $^1J(^{19}F_{A,t}, ^{125}Te_t) = 3501$ Hz, $^1J(^{19}F_{B,t}, ^{125}Te_t) = 3768$ Hz.

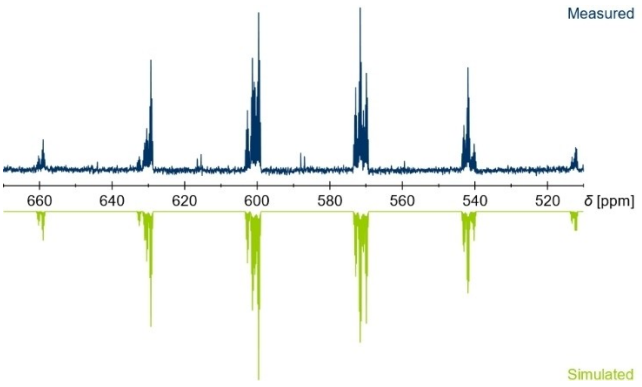

Figure 4. ^{125}Te NMR spectrum (126 MHz, DCM-d_2, 19 °C) of [Au-(CD_3CN)($OTeF_5$)$_3$] (top, blue) compared to the simulated spectrum (bottom, green). NMR spectroscopical parameters used in the simulation for the two –$OTeF_5$ ligands in *cis* position to CD_3CN: $\delta(Te_c) = 586$ ppm, $^1J(^{125}Te_c, ^{19}F_{A,c}) = 3535$ Hz, $^1J(^{125}Te_c, ^{19}F_{B,c}) = 3751$ Hz, $^5J(^{125}Te_c, ^{19}F_{B,t}) = 31$ Hz. NMR spectroscopical parameters used in the simulation for the –$OTeF_5$ ligand in *trans* position to CD_3CN: $\delta(Te_t) = 587$ ppm, $^1J(^{125}Te_t, ^{19}F_{A,t}) = 3501$ Hz, $^1J(^{125}Te_t, ^{19}F_{B,t}) = 3768$ Hz, $^5J(^{125}Te_t, ^{19}F_{B,c}) = 32$ Hz.

Furthermore, the pF^- value was determined ($pF^- =$ FIA[kcal mol^{-1}]/10).[38] The FIAs of the monomer and dimer are 557 ($pF^- = 13.30$) and 504 kJ mol^{-1} ($pF^- = 12.04$), respectively, both being higher than that of SbF_5 (495 kJ mol^{-1}; $pF^- =$ 11.82),[31] which is defined as the border for Lewis superacidity. Furthermore, the reactivity of the monomeric and dimeric Lewis acid towards different ligands L following Scheme 2 was calculated at the RI-BP86/def-SV(P) and RI-B3LYP-D3/def2-TZVPP levels, respectively. The results are summarized in Table 1. It can be seen that the adduct formation with CH_3CN, Et_3PO and Ph_3PO entails in all cases similar reaction energies within a range of about 20 kJ mol^{-1}. Furthermore, all reactions starting from [Au($OTeF_5$)$_3$] listed in Table 1 are about 150 kJ mol^{-1} more exothermic than the dimerization energy of [Au($OTeF_5$)$_3$], supporting the experimental finding that all of these adducts can be synthesized starting from the dimeric Lewis acid.

In order to confirm the classification of [Au($OTeF_5$)$_3$] as a Lewis superacid, its reaction with [PPh_4][SbF_6] in SO_2ClF was investigated with the aim of abstracting a fluoride ion from

$$[Au(OTeF_5)_3] + L \xrightarrow{-\Delta H} [AuL(OTeF_5)_3]$$

Scheme 2. Schematic reaction equation for the calculated reaction energies between [Au($OTeF_5$)$_3$] and different ligands L summarized in Table 1.

[SbF_6]$^-$. The ^{19}F NMR spectrum of the reaction mixture shows a similar pattern to the [Au($OTeF_5$)$_4$]$^-$ anion (see below) and $HOTeF_5$ as a side product, which is only plausible by the initial abstraction of a fluoride ion from [SbF_6]$^-$ and subsequent ligand scrambling. The formation of $HOTeF_5$ probably stems from the reaction of SbF_5 with the cation, yielding HF followed by reaction with the [Au($OTeF_5$)$_4$]$^-$ anion to form $HOTeF_5$. Similar findings have been recently published for the reaction of a solvent adduct of the corresponding aluminum-centered Lewis superacid [Al($OTeF_5$)$_3$(SO_2ClF)$_2$] with [PPh_4][SbF_6].[14] This result is an experimental evidence that [Au($OTeF_5$)$_3$] has a higher FIA than SbF_5 and hence, in addition to the other Lewis acidity measurements, can be classified as a Lewis superacid. This renders [Au($OTeF_5$)$_3$] just the second gold-centered Lewis superacid, after AuF_5. According to calculations of the FIA, AuF_3 is not considered a Lewis superacid, showing that the substitution of fluorides by teflates enhances the FIA and underlines the use of teflate groups for the stabilization of high oxidation states.[7]

Pentafluoroorthotelluratoaurate(III) Anions

In contrast to the Lewis acid, the corresponding homoleptic anion [Au($OTeF_5$)$_4$]$^-$ has not been reported. In order to synthesize it, we first attempted a reaction between [Cat][AuF_4] ([Cat]$^+$ = [NMe_4]$^+$, Cs^+) and $Me_3SiOTeF_5$, since the latter has proven useful in the substitution of fluorides by teflates.[21] However, no [Au($OTeF_5$)$_4$]$^-$ was formed, but [H($OTeF_5$)$_2$]$^-$ was detected as the main product.

Therefore, we changed our starting materials to the corresponding chloride salts [Cat][$AuCl_4$] (Cat$^+$ = Cs^+, [NMe_4]$^+$, [NEt_3Me]$^+$) and used $ClOTeF_5$ as the teflate-transfer reagent, in analogy to the preparation of [Au($OTeF_5$)$_3$] (see above). Preliminary experiments of the reaction between [NMe_4][$AuCl_4$] and $ClOTeF_5$ in DCM resulted in the formation of crystals suitable for X-ray diffraction by cooling down a concentrated solution of the reaction mixture to −16 °C. The crystals were determined to be [NMe_4][$AuCl_3$($OTeF_5$)], as shown in Figure 5. In this structure, the coordination around the gold(III) center is square planar ($\tau_4 = 0.05$). The Au–O bond length is 204.1(4) pm, and hence almost 7 pm longer than in [Au($OPPh_3$)($OTeF_5$)$_3$] (197.3(3) and 197.7(3) pm). This demonstrates the stronger *trans*-influence of the chlorido ligand compared to the teflate ligand, also supported by the fact that the Au–Cl bond *trans* to the oxygen atom is about 4 pm shorter than those of the chlorido ligands *trans* to each other (223.8(2) pm compared to 227.6(2) pm). The latter Au–Cl distance is comparable to those

Table 1. Reaction enthalpies ΔH of the reaction of [Au($OTeF_5$)$_3$] with different ligands L (cf. Scheme 2), calculated at the RI-BP86/def-SV(P) and RI-B3LYP-D3/def2-TZVPP level of theory, respectively; values in kJ mol^{-1}. The fluoride ion affinity (FIA) was calculated using Me_3SiF as anchor point.[31]

L	[Au($OTeF_5$)$_3$]		[Au_2($OTeF_5$)$_6$]	
	RI-BP86/def-SV(P)	RI-B3LYP-D3/def2-TZVPP	RI-BP86/def-SV(P)	RI-B3LYP-D3/def2-TZVPP
F^- (FIA)	−557	−616	−504	−471
CH3CN	−230	−319	−178	−175
Et_3PO	−219	−307	−166	−162
Ph_3PO	−205	−315	−153	−170

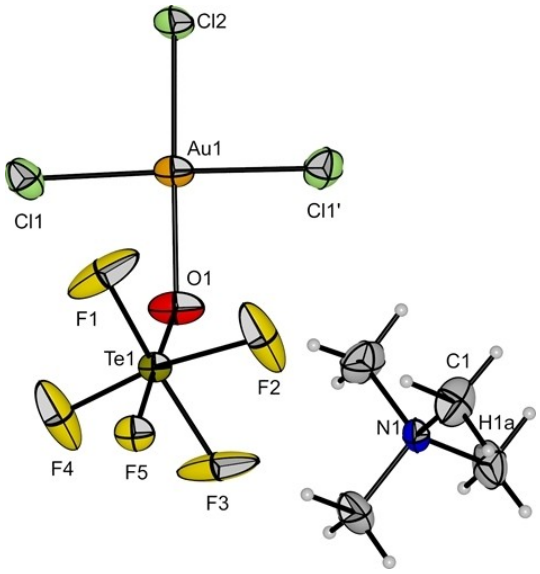

Figure 5. Molecular structure of $[NMe_4][AuCl_3(OTeF_5)]$ in the solid state. Disorders of the basal fluorine atoms (F1–F4) are omitted for clarity (cf. Figure S2). Thermal ellipsoids are shown at 50% probability. Bond lengths [pm] and angles [°] involving the gold atom: 204.1(4) (Au1–O1), 227.6(2) (Au1–Cl1), 223.8(2) (Au1–Cl2); 89.2(3) (O1–Au1–Cl1), 175.3(2) (O1–Au1–Cl2), 178.3(6) (Cl1–Au1–Cl1), 90.8(3) (Cl1–Au1–Cl2).

in $Cs[AuCl_4]$ (227.18(13) pm and 228.38(13) pm).[39] The characterization of the $[AuCl_3(OTeF_5)]^-$ anion supports the postulation of a stepwise substitution going from $[AuCl_4]^-$ to $[Au(OTeF_5)_4]^-$, as indicated by quantum chemical calculations on the RI-B3LYP-D3/def2-TZVPP level, which predict that the first substitution is the most exothermic step with a reaction enthalpy of $\Delta H = -98\ kJ\,mol^{-1}$. For the complete substitution of all chlorides in $[AuCl_4]^-$ by teflate groups yielding $[Au(OTeF_5)_4]^-$, a reaction enthalpy $\Delta H = -317\ kJ\,mol^{-1}$ was calculated (see Scheme S1 and Table S2).

In analogy to the recent preparation of the $[Ni(OTeF_5)_4]^{2-}$ anion by our group, we then changed the approach to using neat $ClOTeF_5$ as shown in Scheme 3.[16] The condensation of $ClOTeF_5$ onto $[NEt_3Me][AuCl_4]$ resulted in a brown slurry that turned into a yellow slurry with a pale yellow gas phase after 3 h. A UV/Vis spectrum of the gas phase confirmed the desired formation of gaseous chlorine (s. Figure S25). Evaporation of all volatile material resulted in a light yellow powder, which was characterized as $[NEt_3Me][Au(OTeF_5)_4]$ (see below).

Single crystals of $[NEt_3Me][Au(OTeF_5)_4]$ suitable for X-ray diffraction were obtained by cooling down a reaction mixture of $[NEt_3Me][AuCl_4]$ and $ClOTeF_5$ in DCM to −16 °C. The salt

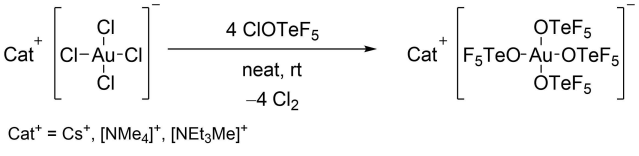

$Cat^+ = Cs^+, [NMe_4]^+, [NEt_3Me]^+$

Scheme 3. Synthetic route to the $[Au(OTeF_5)_4]^-$ anion with different cations starting from the corresponding $[AuCl_4]^-$ salt and an excess of $ClOTeF_5$.

$[NEt_3Me][Au(OTeF_5)_4]$ crystallizes in the orthorhombic space group $P2_12_12_1$. The coordination around the gold(III) center is slightly distorted from the typical square planar arrangement (see Figure 6). The angles α(O–Au–O) involving two oxygen atoms in *cis* position are in a range of 89.5(2)°–90.9(2)°, while α(O–Au–O) with *trans*-oriented oxygen atoms are 169.9(2)° and 171.5(2)°. These angles give a value for the geometry index of $\tau_4 = 0.13$,[35] which is still close to the ideal square planar geometry ($\tau_4 = 0$), but shows even a greater distortion than $[Au(OPPh_3)(OTeF_5)_3]$ (see above). The closest distance between two fluorine atoms of adjacent teflate groups is 300.2(7) pm, which is above the sum of their van der Waals radii. This structural motif is also a minimum structure in quantum chemical calculations on the RI-B3LYP-D3/def2-TZVPP level (cf. Figure S27). Interestingly, the structural motif is different to that of similar, structurally characterized teflate complexes, namely $Xe(OTeF_5)_4$[40] and $[I(OTeF_5)_4]^-$,[36] both having a planar $\{EO_4\}$ unit (E=Xe, I) and adjacent –TeF_5 groups that are oriented pairwise above and below the $\{EO_4\}$ plane. A similar structure to $Xe(OTeF_5)_4$ and $[I(OTeF_5)_4]^-$ is calculated to be a local minimum, but about 1 $kJ\,mol^{-1}$ higher in energy than the structure mentioned above.

The Au–O distances in $[NEt_3Me][Au(OTeF_5)_4]$ are between 196.7(3) pm and 197.7(3) pm, which do not deviate significantly from those in $[Au(OPPh_3)(OTeF_5)_3]$ (197.3(3) pm and 197.7(3) pm, see above), which supports the finding from the previous section that the –$OTeF_5$ group and the –$OPPh_3$ group have a similar *trans*-influence. Compared to the $[AuCl_3(OTeF_5)]^-$ anion (204.1(4) pm), the Au–O bond is about 7 pm shorter, due

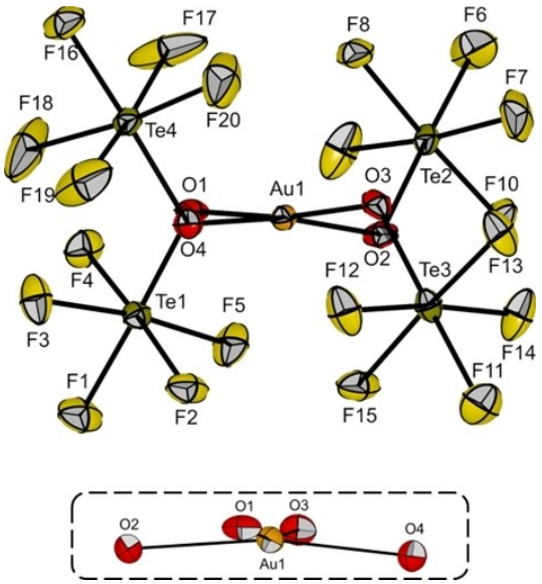

Figure 6. Molecular structure of $[NEt_3Me][Au(OTeF_5)_4]$ in the solid state (top) and excerpt of the $\{AuO_4\}$ unit, highlighting the deviation from a square planar coordination (bottom). The $[NEt_3Me]^+$ cation is omitted for clarity (cf. Figure S1). Thermal ellipsoids are set at 50% probability. Bond lengths [pm] and angles [°] involving the gold atom: 197.4(3) (Au1–O1), 196.7(3) (Au1–O2), 197.7(3) (Au1–O3), 197.2(3) (Au1–O4); 90.8(2) (O1–Au1–O2), 171.5(2) (O1–Au1–O3), 90.9(2) (O1–Au1–O4), 89.5(2) (O2–Au1–O3), 169.9(2) (O2–Au1–O4), 90.2(2) (O3–Au1–O4). The closest F–F distance of two adjacent –$OTeF_5$ groups is 300.2(7) pm (F3–F18).

to the stronger *trans*-influence of the chlorido ligand compared to the teflate ligand (see above). The Au–O distances are also in good agreement with those of the literature-known $[Au(ONO_2)_4]^-$ anion (199(1) pm and 202(2) pm).[41] Furthermore, the Au–O distances are significantly shorter than the E–O distances in $[I(OTeF_5)_4]^-$(208.4(9)-217.4(9) pm)[36] and $Xe(OTeF_5)_4$ (202.6(5)-203.9(5) pm).[40]

Compounds containing the $-OTeF_5$ group often give ^{19}F NMR spectra of higher order with an AB_4X pattern, however, the multiplet patterns can at nowadays common field strengths usually be assigned to the two chemically inequivalent types of fluorine atoms even without a detailed analysis.[42] In the case of the $[Au(OTeF_5)_4]^-$ anion, the chemical shifts δ for the fluorine atom F_A and the fluorine atoms F_B are at −38.5 ppm and −39.5 ppm, respectively, with a coupling constant of $^2J(^{19}F,^{19}F) = 183$ Hz, as determined by simulation of the ^{19}F NMR spectrum (cf. Figure 7). Due to this difference of only 1 ppm, the two multiplets overlap yielding an unusual pattern, which resembles the observed one in the series of $[M(OTeF_5)_6]^-$ (M=As, Sb, Bi) anions, but with an inverted order of the F_A and F_B signals.[43] Note that the pattern of the teflate signals in the ^{19}F and ^{125}Te NMR spectra assigned to the $[Au(OTeF_5)_4]^-$ anion are not significantly influenced by the cation (cf. Figures S13, S14, S17 and S18).

The aforementioned proximity in the chemical shifts of the two different types of fluorine atoms also affects the ^{125}Te NMR spectrum of the $[Au(OTeF_5)_4]^-$ anion. Usually, the ^{125}Te NMR spectrum of compounds containing the $-OTeF_5$ group is of first order showing a doublet of quintets. Hence, a direct determination of the $^1J(^{125}Te,^{19}F)$ coupling constant is usually possible. In contrast, the pattern in the ^{125}Te NMR spectrum of $[Au(OTeF_5)_4]^-$ (cf. Figure 8) resembles only vaguely a doublet of quintets, but it is actually a higher order multiplet and the $^1J(^{125}Te,^{19}F)$ coupling constants cannot be straightforwardly assigned. However, by simulation of the spectrum, the $^1J(^{125}Te,^{19}F)$ coupling constants were determined to be 3280 Hz and 3662 Hz for F_A and F_B, respectively (see Figure 8). The chemical shift of $\delta(^{125}Te) = 587$ ppm is by far the most downfield shifted resonance of all $[E(OTeF_5)_4]^{x-}$ (E=B,[44] Al,[13] C,[46] Te,[46] x = 0, 1) complexes that have been characterized by ^{125}Te NMR spectroscopy so far, as they range from 548 ppm to 569 ppm.

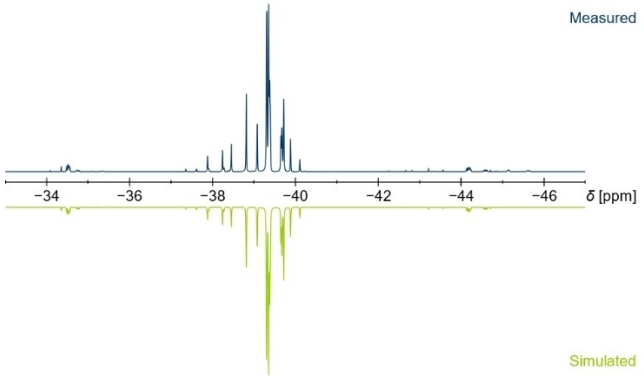

Figure 7. ^{19}F NMR spectrum (377 MHz, DCM-d_2, 17 °C) of $[NEt_3Me][Au(OTeF_5)_4]$ (top, blue) compared to the simulated spectrum (bottom, green). NMR spectroscopical parameters used in the simulation: $\delta(F_A) = -38.5$ ppm, $\delta(F_B) = -39.5$ ppm, $^2J(^{19}F,^{19}F) = 183$ Hz, $^1J(^{19}F_A,^{125}Te) = 3280$ Hz, $^1J(^{19}F_B,^{125}Te) = 3662$ Hz.

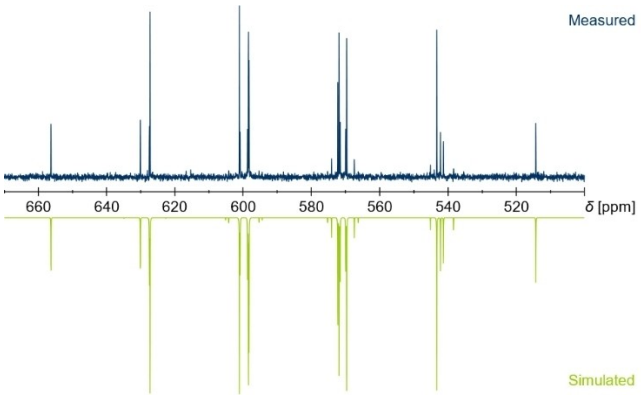

Figure 8. ^{125}Te NMR spectrum (126 MHz, DCM-d_2, 17 °C) of $[NEt_3Me][Au(OTeF_5)_4]$ (top, blue) compared to the simulated spectrum (bottom, green). NMR spectroscopical parameters used in the simulation: $\delta(Te) = 587$ ppm, $^1J(^{125}Te,^{19}F_A) = 3280$ Hz, $^1J(^{125}Te,^{19}F_B) = 3662$ Hz.

In the ESI– mass spectra the parent ion $[Au(OTeF_5)_4]^-$ was not detected, independent of the respective cation, but the gold(I) species $[Au(OTeF_5)_2]^-$ is observed. This anion is an analogue of $[AuF_2]^-$, which has similarly only been detected by mass spectrometry, but never isolated.[47]

The $[Au(OTeF_5)_4]^-$ anion is a rare example of a $\{AuO_4\}$ coordination unit, apart from $[Au(OPPh_3)(OTeF_5)_3]$ (cf. Figure 2), $[Au_2(OTeF_5)_6]$[17] and $[Au(ONO_2)_4]^-$.[41] Solid samples of $[Cat][Au(OTeF_5)_4]$ stored under inert conditions are stable for more than 6 months at room temperature and DCM solutions are stable for several weeks according to ^{19}F NMR spectroscopic investigation. For comparison, the fluorinated analogue $[AuF_4]^-$ is prepared by reacting Au with [Cat][X] ($[Cat]^+ = K^+$, Cs^+, $[NMe_4]^+$, $[NEt_4]^+$; X=F, Cl, Br) in a Br_2/BrF_3 mixture, which is an ambiguous reaction, especially when using organic cations, as explosions may occur.[48]

Due to the aforementioned stability of the $[Au(OTeF_5)_4]^-$ anion and the known ability of the teflate ligand to stabilize high oxidation states,[7] we considered it a suitable precursor for oxidation reactions in search of the first gold(V) species containing other ligands than fluorides. The only literature-known gold(V) compounds are AuF_5[49–51] and the $[AuF_6]^-$ anion with a series of different cations, namely Li^+,[52] $[NO]^+$,[53] $[O_2]^+$,[50–53,54,55] K^+,[52,53] $[KrF]^+$,[49,51] Ag^+,[52] $[IF_6]^+$,[53] $[XeF_5]^+$,[53] $[Xe_2F_{11}]^+$,[53,56] and Cs^+.[52,53,56] First, the oxidation of $[NMe_4][Au(OTeF_5)_4]$ with $Xe(OTeF_5)_2$ in DCM was investigated, but no reaction was observed. Then, diluted F_2 (10% in Ar) was bubbled through a solution of $[NMe_4][Au(OTeF_5)_4]$ in DCM or MeCN at −40 °C. Although a color change was visible, the desired product was not detected. Treatment of the more robust cesium salt $Cs[Au(OTeF_5)_4]$ with neat F_2 in MeCN at −40 °C only led to decomposition. As none of the attempts starting from $[Au(OTeF_5)_4]^-$ showed any hint of oxidation processes happening, we decided to focus on a different approach, by using $CsAuF_6$ as starting material. The use of different transfer reagents was investigated, but unfortunately neither the reaction with neat $ClOTeF_5$, nor with neat $[B(OTeF_5)_3]$

at 60 °C, similar to the procedure of *Seppelt* and co-workers for the preparation of $[Au(OTeF_5)_3]$,[17] led to any gold teflate species so far.

Conclusion

In conclusion, the reaction between commercially available and easy-to-handle gold chlorides and $ClOTeF_5$ arises as a new synthetic route to the Lewis acid $[Au(OTeF_5)_3]$ and its related, unprecedented anion $[Au(OTeF_5)_4]^-$. Adducts of the Lewis acid with Et_3PO, Ph_3PO and CD_3CN were prepared and characterized, being the first compounds containing $[Au(OTeF_5)_3]$ in a monomeric form. Investigation of its Lewis acidity using the Gutmann-Beckett method, analysis of the stretching vibration in its acetonitrile adduct and calculation of the fluoride ion affinity resulted in the classification of $[Au(OTeF_5)_3]$ as a Lewis superacid, being the only known gold Lewis superacid apart from AuF_5. In the solid-state structure of $[Au(OPPh_3)(OTeF_5)_3]$, the gold(III) center shows a unique coordination environment, with an arrangement of the ligands in an alternating way above and below the off-planar $\{AuO_4\}$ unit. A similar structural feature is visible in the solid-state structure of $[NEt_3Me][Au(OTeF_5)_4]$. Furthermore, the $[NMe_4]^+$ and Cs^+ salts of this unprecedented anion were also prepared and characterized, with the ^{19}F NMR spectrum showing an interesting pattern which is due to a difference of only 1 ppm in the chemical shift of the F_A and F_B fluorine atoms. Based on the present work, further reactivity studies of $[Au(OTeF_5)_3]$ and potential applications of $[Au(OTeF_5)_4]^-$ as a weakly coordinating anion could be investigated.

Experimental Section

Materials, Chemicals and Procedures

All experiments were conducted under strict exclusion of moisture and air using standard Schlenk techniques. Solid compounds were handled inside an *MBRAUN UNIlab plus* glovebox with an argon atmosphere ($c(O_2) < 0.5$ ppm, $c(H_2O) < 0.5$ ppm). Solvents were dried using an *MBRAUN SPS-800* solvent system and stored over 4 Å molecular sieves. $ClOTeF_5$[23] and $CsAuF_6$[55] were prepared via literature-known procedures. $[NMe_4][AuCl_4]$, $[NEt_3Me][AuCl_4]$ and $Cs[AuCl_4]$ were prepared by adaptation of the literature-known synthesis of $[NR_4][AuCl_4]$ salts (R=Et, Bu).[57] Raman spectra were recorded at room temperature using a *Bruker MultiRAM* FT-Raman spectrometer with an Nd:YAG laser with 1064 nm wavelength. The samples of the isolated powder material were measured in heat-sealed glass capillaries with a laser power of 30 mW and 256 scans with a resolution of 2 cm^{-1}. Raman spectra of single crystals were recorded at −196 °C using a *Bruker RamanScope III* spectrometer with a Laser power of 450 mW and 256 scans with a resolution of 4 cm^{-1}. The samples were measured using a Teflon plate that is cooled by a liquid nitrogen cooled copper block, producing a nitrogen atmosphere that kept the sample inert.[58] IR spectra were measured at room temperature under an argon stream using a *Nicolet iS50* FTIR spectrometer with a diamond ATR attachment with 32 scans and a resolution of 4 cm^{-1}. For the MIR spectra (4000–400 cm^{-1}), a KBr beam splitter was used, while for the FIR spectra (600–50 cm^{-1}), a polyethylene beam splitter was used. Raman and IR spectra were processed using *OPUS 7.5* and *Origin 2022*[59] was used for their graphical representation. NMR spectra were recorded using a *JEOL 400 MHz ECZ-R* or *ECS* spectrometer and all chemical shifts are referenced using the Ξ values given in the *IUPAC* recommendations of 2008 and the ^2H signal of the deuterated solvent as internal reference.[60] For external locking, acetone-d_6 was flame sealed in a glass capillary and the lock oscillator frequency was adjusted to give $\delta(^1H) = 7.26$ ppm for a $CHCl_3$ sample locked on the capillary. For strongly coupled spin systems all chemical shifts and coupling constants are reported as simulated in *gNMR*.[61] *MestReNova 14.2* was used for processing the spectra and for their graphical representation. X-ray diffraction measurements were performed on a *Bruker D8 Venture* diffractometer with MoK_α ($\lambda = 0.71073$ Å) radiation at 100 K and powder X-ray diffraction measurements were performed on a *Bruker D8 Venture* diffractometer with CuK_α ($\lambda = 1.54184$ Å) radiation at 293 K. Single crystals were picked in perfluoroether oil at −40 °C under a nitrogen atmosphere and mounted on a 0.15 mm *Mitegen* micromount. They were solved using the *ShelXT*[62] structure solution program with intrinsic phasing and were refined with the refinement package *ShelXL*[63] using least squares minimizations by using the program *OLEX2*.[64] *Diamond 3* and *POV-Ray 3.7* were used for their graphical representation. UV spectra were measured using a *LAMBDA 465* UV/Vis spectrophotometer. ESI mass spectra were recorded using an *Agilent 6210 ESI-TOF* mass spectrometer, with a flow rate of 4 μL min^{-1} and a spray voltage of 4 kV. The gas for desolvation was set to 1 bar. Elemental analyses (CHN) were performed using a *vario EL* elemental analyzer. Quantum chemical calculations were performed using the functionals B3LYP[65] or BP86 with RI[66] and Grimme-D3[67] corrections where indicated and the basis sets def2-TZVPP[68] or def-SV(P)[69] as incorporated in *TURBOMOLE V7.3*.[70] Reaction enthalpies were calculated by subtraction of the enthalpies of the starting materials from the ones of the products, which were obtained from the calculated SCF energy of geometry optimized minimum structures that were corrected for the enthalpy at standard temperature and pressure using the module *freeh* as incorporated in *TURBOMOLE V7.3* with scaling factors of 0.9614 and 0.9914 for B3LYP and BP86, respectively.[70]

Preparation of $[Au(OTeF_5)_3]$: $ClOTeF_5$ (818 mg, 2.98 mmol, 9 equiv.) was condensed onto a sample of $AuCl_3$ (103 mg, 0.340 mmol, 1 equiv.). The mixture was slowly warmed to room temperature and stirred for 16 h, resulting in an orange-red solution with an orange solid. Volatiles were removed under reduced pressure and afterwards trapped under reduced, static pressure at −80 °C to separate $ClOTeF_5$ from the formed Cl_2. The remaining $ClOTeF_5$ was condensed back onto the reaction mixture and the mixture was stirred for 3 h. All volatiles were removed under reduced pressure and fresh $ClOTeF_5$ (245 mg, 0.894 mmol, 3 equiv.) was condensed onto the reaction mixture and stirred for 3 h. All volatiles were removed under reduced pressure. The product (310 mg, 0.339 mmol, quant.) was obtained as an orange powder. IR (ATR, 25 °C, 4 cm^{-1}): $\tilde{\nu} = 772$ (m, ν_{as}(Au–O)), 691 (vs, ν_{as}(Te–F_B)), 635 (m, ν_{as}(Te–F_A)), 509 (m, $\delta_{ring,oop}(Au_2O_2)$), 297 (vs, δ_{oop}(Te–F_B)), 235 (s, δ_{ip}(Te–F_B)), 156 (m, δ_{ip}(O–Te–F_A)), 92 (m, δ_{oop}(Au–O–Te–F_A)), 81 (m, δ_{ip}(Au–O–Te–F_A)), 73 (m, δ_{ip}(Au–O–Te)), 56 (m) cm^{-1}. FT-Raman (25 °C, 30 mW, 2 cm^{-1}): $\tilde{\nu} = 815$ (m, ν_s(Au–O)), 754 (m, ν_{as}(Au–O)), 732 (m, ν_{as}(Te–F_B)), 725 (m, ν_{as}(Te–F_B)), 715 (m, ν_{as}(Te–F_B)), 702 (s, ν_{as}(Te–F_B)), 669 (vs, ν_s(Te–F_B)), 652 (m, ν_s(Te–F_B)), 637 (m, ν_s(Te–F_B)), 530 (s, $\delta_{ring,ip}(Au_2O_2)$), 493 (m, $\delta_{ring,oop}(Au_2O_2)$), 402 (m, δ_{oop}(Au–O–Au), 326 (m, δ_{oop}(Te–F_B)), 308 (m, δ_{oop}(Te–F_B)), 244 (m, δ_{ip}(Te–F_B)), 228 (m, δ_{ip}(Te–F_B)), 192 (w, δ_{oop}(O–Te–F_B)), 171 (w, δ_{ip}(O–Te–F_A)), 142 (s, δ_{oop}(Au–O–Te–F_A)), 136 (vs, δ_{oop}(Au–O–Te–F_A)), 121 (m, δ_{oop}(O–Te–F_A)), 106 (m, δ_{oop}(O–Te–F_A)), 94 (s, δ_{oop}(Au–O–Te–F_A)), 69 (s) cm^{-1}.

Preparation of [Au(OPEt$_3$)(OTeF$_5$)$_3$]: Et_3PO (12 mg, 0.0894 mmol, 2.3 equiv.) was added to a suspension of [Au(OTeF$_5$)$_3$] (36 mg, 0.0394 mmol, 1 equiv.) in DCM-d$_2$ (1 mL). The mixture was stirred at −40 °C for 2 h, yielding a clear, yellow solution. ^{1}H NMR (400 MHz, DCM-d$_2$, 21 °C): δ = 2.38 (m, 6H, –CH$_2$), 1.24 (m, 9H, –CH$_3$) ppm. ^{19}F NMR (377 MHz, DCM-d$_2$, 21 °C): δ = −37.8 (m), −38.5 (m) ppm. ^{31}P{^{1}H} NMR (162 MHz, DCM-d$_2$, 21 °C): δ = 106.1 (s) ppm.

Preparation of [Au(OPPh$_3$)(OTeF$_5$)$_3$]: Ph_3PO (9 mg, 0.0323 mmol, 1 equiv.) was added to a suspension of [Au(OTeF$_5$)$_3$] (30 mg, 0.0329 mmol, 1 equiv.) in DCM-d$_2$ (1 mL). The mixture was stirred at room temperature for 10 minutes, yielding a clear, yellow solution. ^{1}H NMR (400 MHz, DCM-d$_2$, 19 °C): δ = 7.90–7.55 (m, –H$_{ar}$) ppm. ^{19}F NMR (377 MHz, DCM-d$_2$, 19 °C): δ = −38.7 (m), −39.3 (m) ppm. ^{31}P{^{1}H} NMR (162 MHz, DCM-d$_2$, 19 °C): δ = 66.5 (s) ppm.

Preparation of [Au(CD$_3$CN)(OTeF$_5$)$_3$]: CD_3CN (2.2 µL, 0.0389 mmol, 1 equiv.) was added to a suspension of [Au(OTeF$_5$)$_3$] (35 mg, 0.0383 mmol, 1 equiv.) in DCM-d$_2$ (1 mL). The mixture was stirred at room temperature for 5 minutes, yielding a clear, bright orange solution. For the IR measurements, all volatiles were pumped off, resulting in a red solid. **^{19}F NMR** (377 MHz, DCM-d$_2$, 20 °C): δ = −43.5 (m, 1F$_{A,c}$, $^2J(^{19}F_{A,c},^{19}F_{B,c})$ = 182 Hz, $^1J(^{19}F_{A,c},^{125}Te_c)$ = 3501 Hz), −44.5 (m, 2F$_{A,t}$, $^2J(^{19}F_{A,t},^{19}F_{B,t})$ = 181 Hz, $^1J(^{19}F_{A,t},^{125}Te_t)$ = 3535 Hz), −49.1 (m, 8F$_{B,c}$, $^1J(^{19}F_{B,c},^{125}Te_c)$ = 3751 Hz, $^5J(^{19}F_{B,c},^{125}Te_t)$ = 32 Hz), −49.3 (m, 4F$_{B,t}$, $^1J(^{19}F_{B,t},^{125}Te_t)$ = 3768 Hz, $^5J(^{19}F_{B,t},^{125}Te_c)$ = 31 Hz) ppm. ^{125}Te NMR (126 MHz, DCM-d$_2$, 19 °C): δ = 587 (m, 1Te$_t$, $^1J(^{19}F_{A,t},^{125}Te_t)$ = 3501 Hz, $^1J(^{19}F_{B,t},^{125}Te_t)$ = 3768 Hz, $^5J(^{19}F_{B,c},^{125}Te_t)$ = 32 Hz), 586 (m, 2Te$_c$, $^1J(^{19}F_{A,c},^{125}Te_c)$ = 3535 Hz, $^1J(^{19}F_{B,c},^{125}Te_c)$ = 3751 Hz, $^5J(^{19}F_{B,t},^{125}Te_c)$ = 31 Hz) ppm. IR (ATR, 25 °C, 4 cm^{-1}): $\tilde{\nu}$ = 2335 (m, ν(N≡C)), 2262 (vw, ν_{as}(C–H)), 2212 (vw, ν_{as}(C–H)), 2115 (vw, ν_s(C–H)), 1670 (vw), 1590 (vw), 1394 (vw), 1245 (vw), 1156 (vw), 1122 (vw), 1083 (w, δ_{oop}(C–H)), 998 (vw, δ_{ip}(C–H)), 816 (m, ν_s(Au–O)), 782 (m, ν_{as}(Au–O)), 670 (vs, ν_{as}(Te–F$_B$)), 563 (m, $\nu_{as}(\nu_s$(Te–F$_B$) + ν_s(O–Te–F$_A$))), 409 (w, δ_{ip}(N–C–C–H)) cm^{-1}.

Reaction between [Au(OTeF$_5$)$_3$] and [PPh$_4$][SbF$_6$]: [Au(OTeF$_5$)$_3$] (21 mg, 0.0230 mmol, 1 equiv.) and [PPh$_4$][SbF$_6$] (13 mg, 0.0226 mmol, 1 equiv.) were suspended in SO_2ClF (1 mL) at room temperature and agitated for 30 minutes, yielding an orange solution and a colorless solid. The reaction mixture was analyzed by NMR spectroscopy. ^{1}H NMR (400 MHz, SO_2ClF, ext. acetone-d$_6$, 23 °C): δ = 6.75 (m, 4H, *para*–CH), 6.59 (m, 8H, *meta*–CH), 6.48 (m, 8H, *ortho*–CH), 5.24 (s, 1H, HOTeF$_5$) ppm. ^{19}F NMR (377 MHz, SO_2ClF, ext. acetone-d$_6$, 22 °C): δ = −40.7 (m, 1F$_A$, [Al(OTeF$_5$)$_4$]$^-$, $^2J(^{19}F_A,^{19}F_B)$ = 181 Hz), −41.8 (m, 4F$_B$, [Al(OTeF$_5$)$_4$]$^-$), −45.7 (m, 1F$_A$, HOTeF$_5$, $^2J(^{19}F_A,^{19}F_B)$ = 180 Hz), −49.4 (m, 4F$_B$, HOTeF$_5$, $^1J(^{19}F_B,^{125}Te)$ = 3583 Hz) ppm. ^{31}P{^{1}H} NMR (162 MHz, SO_2ClF, ext. acetone-d$_6$, 23 °C): δ = 22.3 (s, 1P, [PPh$_4$]$^+$) ppm.

Preparation of [NMe$_4$][Au(OTeF$_5$)$_4$]: $ClOTeF_5$ (642 mg, 2.34 mmol, 10 equiv.) was condensed onto a sample of [NMe$_4$][AuCl$_4$] (98 mg, 0.237 mmol, 1 equiv.). The mixture was slowly warmed to room temperature, resulting in a yellow solution with a light brown solid. The mixture was stirred for 3 h, yielding a light yellow solid with a yellow liquid and a slightly yellow gas phase. All volatiles were removed under reduced pressure. The product (291 mg, 0.234 mmol, quant.) was obtained as a light yellow powder. ^{1}H NMR (400 MHz, DCM-d$_2$, 19 °C): δ = 3.20 (s, 12H, –CH$_3$) ppm. ^{13}C{^{1}H} NMR (101 MHz, DCM-d$_2$, 21 °C): δ = 57.1 (t, 4 C, –CH$_3$, $^1J(^{13}C,^{14}N)$ = 4 Hz) ppm. ^{19}F NMR (377 MHz, DCM-d$_2$, 20 °C): δ = −38.4 (m, 1F$_A$, $^2J(^{19}F,^{19}F)$ = 183 Hz, $^1J(^{19}F,^{125}Te)$ = 3282 Hz), −39.4 (m, 4F$_B$, $^1J(^{19}F,^{125}Te)$ = 3663 Hz) ppm. ^{125}Te NMR (126 MHz, DCM-d$_2$, 19 °C): δ = 586 (m, 1Te, $^1J(^{19}F,^{125}Te)$ = 3282 Hz, $^1J(^{19}F,^{125}Te)$ = 3663 Hz) ppm. IR (ATR, 25 °C, 4 cm^{-1}): $\tilde{\nu}$ = 1486 (m, δ_{ip}(C–H)), 950 (w, ν_{as}(N–C)), 778 (s, ν_{as}(Au–O)), 692 (vs, ν_{as}(Te–F$_B$)), 679 (vs, ν(Te–F$_A$)), 631 (m, ν_{as} (ν_s(Te–F$_B$) + ν_s(O–Te–F$_A$))), 514 (w, δ_{oop}(Au–O)), 307 (vs, δ_{oop}(Te–F$_B$)), 232 (w, δ_{ip}(Te–F$_B$)), 168 (w, δ_{ip}(O–Te–F$_A$)), 71 (s, δ_{ip}(Au–O–Te–F$_A$)), 55 (vs) cm^{-1}. FT-Raman (25 °C, 30 mW, 2 cm^{-1}): $\tilde{\nu}$ = 3047 (m, ν_s(C–H)), 2990 (s, ν_s(C–H)), 2964 (m, ν_s(C–H)), 2931 (m, ν_s(C–H)), 1453 (m, δ_{ip}(C–H)), 755 (m, ν_s(N–C)), 703 (vs, ν_{as}(Te–F)), 688 (s, ν_{as}(Te–F)), 645 (vs, ν_s(Te–F)), 514 (vs, δ_{ip}(Au–O)), 300 (m, δ_{ip}(Te–F)), 235 (s, δ_{ip}(Te–F)), 135 (vs, δ_{oop}(Te–F)), 90 (s, δ_{ip}(Au–O–Te)) cm^{-1}. MS (ESI−): *m/z* = 966.918 (impurity from the spectrometer, 100 %), 674.758 ([Au(OTeF$_5$)$_2$]$^-$, 1.7 %), 500.780 ([Na(OTeF$_5$)$_2$]$^-$, calc. 500.772, 2.8 %), 240.896 ([OTeF$_5$]$^-$, calc. 240.891, 75.5 %), 224.901 ([TeF$_5$]$^-$, calc. 224.896, 56.4 %) Da. Elemental analysis [%]: calculated for $C_4H_{12}AuF_{20}NO_4Te_4$: C 3.92, H 0.99, N 1.14; found: C 4.07, H 1.08, N 1.14.

Preparation of [NEt$_3$Me][Au(OTeF$_5$)$_4$]: Following the procedure for the synthesis of [NMe$_4$][Au(OTeF$_5$)$_4$], [NEt$_3$Me][Au(OTeF$_5$)$_4$] was prepared from $ClOTeF_5$ (556 mg, 2.03 mmol, 10 equiv.) and [NEt$_3$Me][AuCl$_4$] (92 mg, 0.202 mmol, 1 equiv.) yielding [NEt$_3$Me][Au(OTeF$_5$)$_4$] as a light yellow powder (257 mg, 0.202 mmol, quant.). ^{1}H NMR (400 MHz, DCM-d$_2$, 18 °C): δ = 3.23 (q, 6H, –*CH*$_2$CH$_3$, $^2J(^1H,^1H)$ = 7 Hz), 2.88 (s, 3H, –CH$_3$), 1.38 (tt, 9H, –CH$_2$*CH*$_3$, $^3J(^1H,^{14}N)$ = 2 Hz) ppm. ^{13}C{^{1}H} NMR (101 MHz, DCM-d$_2$, 19 °C): δ = 57.0 (t, 3 C, –*CH*$_2$CH$_3$, $^1J(^{13}C,^{14}N)$ = 3 Hz), 47.6 (t, 1 C, –CH$_3$, $^1J(^{13}C,^{14}N)$ = 4 Hz), 8.0 (s, 3 C, –CH$_2$*CH*$_3$) ppm. ^{19}F NMR (377 MHz, DCM-d$_2$, 17 °C): δ = −38.5 (m, 1F$_A$, $^2J(^{19}F,^{19}F)$ = 183 Hz, $^1J(^{19}F,^{125}Te)$ = 3280 Hz), −39.5 (m, 4F$_B$, $^1J(^{19}F,^{125}Te)$ = 3662 Hz) ppm. ^{125}Te NMR (126 MHz, DCM-d$_2$, 17 °C): δ = 585 (m, 1Te, $^1J(^{19}F,^{125}Te)$ = 3280 Hz, $^1J(^{19}F,^{125}Te)$ = 3662 Hz) ppm. IR (ATR, 25 °C, 4 cm^{-1}): $\tilde{\nu}$ = 1488 (vw, δ_{ip}(C–H)), 1460 (vw, δ_{oop}(C–H)), 1448 (vw, δ_{oop}(C–H)), 1397 (vw, δ_{oop}(C–H)), 1191 (vw, δ_{ip}(N–C–C)), 998 (vw, ν_{as}(C–C)), 806 (m, δ_{ip}(C–H)), 774 (s, ν_{as}(Au–O)), 695 (vs, ν_{as}(Te–F$_B$)), 681 (vs, ν(Te–F$_A$)), 630 (m, $\nu_{as}(\nu_s$(Te–F$_B$) + ν_s(O–Te–F$_A$))), 521 (m, δ_{oop}(Au–O)), 307 (vs, δ_{oop}(Te–F$_B$)), 248 (m), 235 (m, δ_{ip}(Te–F$_B$)), 168 (m, δ_{ip}(O–Te–F$_A$)), 142 (w), 67 (m, δ_{ip}(Au–O–Te–F$_A$)), 61 (m) cm^{-1}. FT-Raman (25 °C, 30 mW, 2 cm^{-1}): $\tilde{\nu}$ = 2991 (m, ν_s(C–H)), 2964 (m, ν_s(C–H)), 1462 (m, δ_{ip}(C–H)), 704 (s, ν_{as}(Te–F)), 691 (s, ν_{as}(Te–F)), 645 (vs, ν_s(Te–F)), 519 (vs, δ_{ip}(Au–O)), 336 (m, δ_{ip}(Te–F)), 299 (m, δ_{ip}(Te–F)), 238 (s, (m, δ_{ip}(Te–F)), 137 (vs, δ_{oop}(Te–F)), 96 (s, δ_{ip}(Au–O–Te)) cm^{-1}. MS (ESI−): *m/z* = 966.918 (impurity from the spectrometer, 93.2 %), 674.756 ([Au(OTeF$_5$)$_2$]$^-$, calc. 674.749, 0.6 %), 500.779 ([Na(OTeF$_5$)$_2$]$^-$, calc. 500.772, 4.0 %), 240.896 ([OTeF$_5$]$^-$, calc. 240.891, 100 %), 224.900 ([TeF$_5$]$^-$, calc. 224.896, 69.0 %) Da. Elemental analysis [%]: calculated for $C_7H_{18}AuF_{20}NO_4Te_4$: C 6.63, H 1.43, N 1.11; found: C 6.77, H 1.60, N 1.34.

Preparation of Cs[Au(OTeF$_5$)$_4$]: Following the procedure for the synthesis of [NMe$_4$][Au(OTeF$_5$)$_4$], Cs[Au(OTeF$_5$)$_4$] was prepared from $ClOTeF_5$ (407 mg, 1.49 mmol, 10 equiv.) and Cs[AuCl$_4$] (71 mg, 0.151 mmol, 1 equiv.) yielding Cs[Au(OTeF$_5$)$_4$] as a light yellow powder (161 mg, 0.125 mmol, 83 %). ^{19}F NMR (377 MHz, DCM-d$_2$, 19 °C): δ = −37.9 (m, 1F$_A$, $^2J(^{19}F,^{19}F)$ = 183 Hz, $^1J(^{19}F,^{125}Te)$ = 3309 Hz), −38.9 (m, 4F$_B$, $^1J(^{19}F,^{125}Te)$ = 3662 Hz) ppm. ^{125}Te NMR (126 MHz, DCM-d$_2$, 19 °C): δ = 585 (m, 1Te, $^1J(^{19}F,^{125}Te)$ = 3309 Hz, $^1J(^{19}F,^{125}Te)$ = 3662 Hz) ppm. ^{133}Cs NMR (53 MHz, DCM-d$_2$, 19 °C): δ = 5 (s) ppm. IR (ATR, 25 °C, 4 cm^{-1}): $\tilde{\nu}$ = 872 (m), 825 (m), 792 (m, ν_{as}(Au–O)), 698 (s, ν_{as}(Te–F$_B$)), 676 (s, ν(Te–F$_A$)), 635 (s, $\nu_{as}(\nu_s$(Te–F$_B$) + ν_s(O–Te–F$_A$))), 525 (w), 501 (m, δ_{oop}(Au–O)), 476 (w), 460 (vw), 386 (vw), 308 (vs, δ_{oop}(Te–F$_B$)), 234 (m, δ_{ip}(Te–F$_B$)), 183 (w), 167 (w, δ_{ip}(O–Te–F$_A$)), 145 (w), 135 (w), 107 (w), 88 (m), 68 (s, δ_{ip}(Au–O–Te–F$_A$)), 63 (s), 58 (s) cm^{-1}. FT-Raman (25 °C, 30 mW, 2 cm^{-1}): $\tilde{\nu}$ = 871 (w, ν_s(Au–O)), 683 (m, ν_{as}(Te–F)), 650 (m, ν(Te–F)), 579 (w), 388 (s), 352 (vs), 333 (s, δ_{ip}(Te–F)), 323 (vs), 181 (s), 142 (m, δ_{oop}(Te–F)), 108 (m, δ_{ip} (Au–O–Te))), 77 (s) cm^{-1}. MS (ESI−): *m/z* = 966.919 (impurity from the spectrometer, 100 %), 500.780 ([Na(OTeF$_5$)$_2$]$^-$, calc. 500.772, 1.5 %), 240.899 ([OTeF$_5$]$^-$, calc. 240.891, 10.7 %), 224.904 ([TeF$_5$]$^-$, calc. 224.896, 10.5 %) Da.

Deposition Numbers 2173738, 2156160, 2156159 contain the supplementary crystallographic data for this paper. These data are provided free of charge by the joint Cambridge Crystallographic

Data Centre and Fachinformationszentrum Karlsruhe Access Structures service.

Acknowledgements

Funded by the ERC project HighPotOx (Grant agreement ID:818862). The authors would like to thank the HPC Service of ZEDAT, Freie Universität Berlin, for computing time and gratefully acknowledge the assistance of the Core Facility BioSupraMol supported by the DFG. M.W. thanks the Dahlem Research School for financial support. A.P.B. and M.A.E. thank the Alexander von Humboldt Foundation for a postdoctoral research fellowship. Open Access funding enabled and organized by Projekt DEAL.

Conflict of Interest

The authors declare no conflict of interest.

Data Availability Statement

The data that support the findings of this study are available from the corresponding author upon reasonable request.

Keywords: gold · lewis acidity · lewis superacid · ligand affinity · pentafluoroorthotellurate

[1] G. N. Lewis, *Valence and the Structure of Atoms and Molecules*, The Chemical Catalog Company, Inc., New York, **1923**.
[2] a) H. Yamamoto, *Lewis Acids in Organic Synthesis*, Wiley-VCH Verlag GmbH, Weinheim, Germany, **2000**; b) A. Corma, H. García, *Chem. Rev.* **2003**, *103*, 4307.
[3] L. O. Müller, D. Himmel, J. Stauffer, G. Steinfeld, J. Slattery, G. Santiso-Quiñones, V. Brecht, I. Krossing, *Angew. Chem. Int. Ed.* **2008**, *47*, 7659; *Angew. Chem.* **2008**, *120*, 7772.
[4] J. F. Kögel, D. A. Sorokin, A. Khvorost, M. Scott, K. Harms, D. Himmel, I. Krossing, J. Sundermeyer, *Chem. Sci.* **2018**, *9*, 245.
[5] L. A. Körte, J. Schwabedissen, M. Soffner, S. Blomeyer, C. G. Reuter, Y. V. Vishnevskiy, B. Neumann, H.-G. Stammler, N. W. Mitzel, *Angew. Chem. Int. Ed.* **2017**, *56*, 8578; *Angew. Chem.* **2017**, *129*, 8701.
[6] L. Greb, *Chem. Eur. J.* **2018**, *24*, 17881.
[7] K. Seppelt, *Angew. Chem. Int. Ed.* **1982**, *21*, 877; *Angew. Chem.* **1982**, *94*, 890.
[8] a) P. K. Hurlburt, D. M. Van Seggen, J. J. Rack, S. H. Strauss in *ACS Symposium Series* (Hrsg.: K. K. Laali), American Chemical Society, Washington, DC, **2007**, S. 338–349; b) M. Gerken, H. P. A. Mercier, G. J. Schrobilgen in *Advanced Inorganic Fluorides; Synthesis, Characterization and Applications* (Hrsg.: T. Nakajima, B. Zemva, A. Tressaud), Elsevier Science S. A. Lausanne, Switzerland, **2000**, S. 117–174.
[9] D. Lentz, K. Seppelt, *Z. Anorg. Allg. Chem.* **1983**, *502*, 83.
[10] M. J. Collins, G. J. Schrobilgen, *Inorg. Chem.* **1985**, *24*, 2608.
[11] F. Sladky, *Monatsh. Chem.* **1970**, *101*, 1559.
[12] a) K. Seppelt, *Chem. Ber.* **1976**, *109*, 1046; b) L. K. Templeton, D. H. Templeton, N. Bartlett, K. Seppelt, *Inorg. Chem.* **1976**, *15*, 2720.
[13] A. Wiesner, T. W. Gries, S. Steinhauer, H. Beckers, S. Riedel, *Angew. Chem. Int. Ed.* **2017**, *56*, 8263; *Angew. Chem.* **2017**, *129*, 8375.
[14] K. F. Hoffmann, A. Wiesner, S. Steinhauer, S. Riedel, *Chem. Eur. J.* **2022**, e202201958.
[15] A. Wiesner, S. Steinhauer, H. Beckers, C. Müller, S. Riedel, *Chem. Sci.* **2018**, *9*, 7169.
[16] A. Pérez-Bitrián, K. F. Hoffmann, K. B. Krause, G. Thiele, C. Limberg, S. Riedel, *Chem. Eur. J.* **2022**, e202202016.
[17] P. Huppmann, H. Hartl, K. Seppelt, *Z. Anorg. Allg. Chem.* **1985**, *524*, 26.
[18] F. W. B. Einstein, P. R. Rao, J. Trotter, N. Bartlett, *J. Chem. Soc. A* **1967**, 478.
[19] D. R. Lide, *ed.*, *CRC Handbook of Chemistry and Physics*, 87. Aufl., Taylor & Francis, Boca Raton, FL., **2006**, p 9–54.
[20] W. J. Wolf, F. D. Toste in *Patai's chemistry of functional groups* (Hrsg.: Z. Rappoport, J. F. Liebman, I. Marek), Wiley, Chichester, **2014**, S. 391–408.
[21] M. A. Ellwanger, C. Von Randow, S. Steinhauer, Y. Zhou, A. Wiesner, H. Beckers, T. Braun, S. Riedel, *Chem. Commun.* **2018**, *54*, 9301.
[22] K. Seppelt, D. Nothe, *Inorg. Chem.* **1973**, *12*, 2727.
[23] C. J. Schack, K. O. Christe, *J. Fluorine Chem.* **1982**, *21*, 393.
[24] a) L. Turowsky, K. Seppelt, *Z. Anorg. Allg. Chem.* **1990**, *590*, 23; b) L. Turowsky, K. Seppelt, *Z. Anorg. Allg. Chem.* **1990**, *590*, 37; c) T. Drews, K. Seppelt, *Z. Anorg. Allg. Chem.* **1991**, *606*, 201; d) A. Vij, W. W. Wilson, V. Vij, R. C. Corley, F. S. Tham, M. Gerken, R. Haiges, S. Schneider, T. Schroer, R. I. Wagner, *Inorg. Chem.* **2004**, *43*, 3189.
[25] U. Mayer, V. Gutmann, W. Gerger, *Monatsh. Chem.* **1975**, *106*, 1235.
[26] M. A. Beckett, G. C. Strickland, J. R. Holland, K. Sukumar Varma, *Polymer* **1996**, *37*, 4629.
[27] D. M. Byler, D. F. Shriver, *Inorg. Chem.* **1973**, *12*, 1412.
[28] D. M. Byler, D. F. Shriver, *Inorg. Chem.* **1974**, *13*, 2697.
[29] B. V. Ahsen, B. Bley, S. Proemmel, R. Wartchow, H. Willner, F. Aubke, *Z. Anorg. Allg. Chem.* **1998**, *624*, 1225.
[30] J. C. Haartz, D. H. McDaniel, *J. Am. Chem. Soc.* **1973**, *95*, 8562.
[31] H. Böhrer, N. Trapp, D. Himmel, M. Schleep, I. Krossing, *Dalton Trans.* **2015**, *44*, 7489.
[32] A. Pérez-Bitrián, M. Baya, J. M. Casas, L. R. Falvello, A. Martín, B. Menjón, *Chem. Eur. J.* **2017**, *23*, 14918.
[33] N. Burford, B. W. Royan, R. E. V. H. Spence, T. S. Cameron, A. Linden, R. D. Rogers, *J. Chem. Soc. Dalton Trans.* **1990**, 1521.
[34] H. Großekappenberg, M. Reißmann, M. Schmidtmann, T. Müller, *Organometallics* **2015**, *34*, 4952.
[35] L. Yang, D. R. Powell, R. P. Houser, *Dalton Trans.* **2007**, 955.
[36] L. Turowsky, K. Seppelt, *Z. Anorg. Allg. Chem.* **1991**, *602*, 79.
[37] W. R. Fawcett, G. Liu, T. E. Kessler, *J. Phys. Chem.* **1993**, *97*, 9293.
[38] K. O. Christe, D. A. Dixon, D. McLemore, W. W. Wilson, J. A. Sheehy, J. A. Boatz, *J. Fluorine Chem.* **2000**, *101*, 151.
[39] F. Kraus, *Z. Naturforsch. B. Chem. Sci.* **2011**, *66*, 871.
[40] L. Turowsky, K. Seppelt, *Z. Anorg. Allg. Chem.* **1992**, *609*, 153.
[41] C. D. Garner, S. C. Wallwork, *J. Chem. Soc. A* **1970**, 3092.
[42] K. Seppelt, *Z. Anorg. Allg. Chem.* **1973**, *399*, 65.
[43] H. P. A. Mercier, J. C. P. Sanders, G. J. Schrobilgen, *J. Am. Chem. Soc.* **1994**, *116*, 2921.
[44] H. Kropshofer, O. Leitzke, P. Peringer, F. Sladky, *Chem. Ber.* **1981**, *114*, 2644.
[45] M. D. Moran, H. P. A. Mercier, G. J. Schrobilgen, *Inorg. Chem.* **2007**, *46*, 5034.
[46] T. Birchall, R. D. Myers, H. D. Waard, G. J. Schrobilgen, *Inorg. Chem.* **1982**, *21*, 1068.
[47] a) N. J. Rijs, R. A. J. O'Hair, *Dalton Trans.* **2012**, *41*, 3395; b) A. Pérez-Bitrián, M. Baya, J. M. Casas, A. Martín, B. Menjón, J. Orduna, *Angew. Chem. Int. Ed.* **2018**, *57*, 6517; *Angew. Chem.* **2018**, *130*, 3425.
[48] a) A. G. Sharpe, *J. Chem. Soc.* **1949**, 2901; b) M. A. Ellwanger, S. Steinhauer, P. Golz, H. Beckers, A. Wiesner, B. Braun-Cula, T. Braun, S. Riedel, *Chem. Eur. J.* **2017**, *23*, 13501.
[49] J. H. Holloway, G. J. Schrobilgen, *J. Chem. Soc. Chem. Commun.* **1975**, 623.
[50] M. J. Vasile, T. J. Richardson, F. A. Stevie, W. E. Falconer, *J. Chem. Soc. Dalton Trans.* **1976**, 351.
[51] I.-C. Hwang, K. Seppelt, *Angew. Chem. Int. Ed.* **2001**, *40*, 3690; *Angew. Chem.* **2001**, *113*, 3803.
[52] O. Graudejus, S. H. Elder, G. M. Lucier, C. Shen, N. Bartlett, *Inorg. Chem.* **1999**, *38*, 2503.
[53] N. Bartlett, *Rev. Chim. Miner.* **1976**, *13*, 82.
[54] a) O. Graudejus, B. G. Müller, *Z. Anorg. Allg. Chem.* **1996**, *622*, 1076; b) J. E. Griffiths, W. A. Sunder, W. E. Falconer, *Spectrochim. Acta Part A* **1975**, *31*, 1207; c) A. J. Edwards, W. E. Falconer, J. E. Griffiths, W. A. Sunder, M. J. Vasile, *J. Chem. Soc. Dalton Trans.* **1974**, 1129; d) Z. Mazej, E. Goreshnik, *Inorg. Chem.* **2020**, *59*, 2092.
[55] Z. Mazej in *Modern Synthesis Processes and Reactivity of Fluorinated Compounds. Progress in Fluorine Science* (Hrsg.: H. Groult, F. Leroux, A. Tressaud), Elsevier Science, San Diego, CA, USA, **2016**, S. 587–607.
[56] K. Leary, N. Bartlett, *J. Chem. Soc. Chem. Commun.* **1972**, 903.

[57] P. Braunstein, R. J. H. Clark, *J. Chem. Soc. Dalton Trans.* **1973**, 1845.
[58] P. Voßnacker, T. Keilhack, N. Schwarze, K. Sonnenberg, K. Seppelt, M. Malischewski, S. Riedel, *Eur. J. Inorg. Chem.* **2021**, *2021*, 1034.
[59] OriginLab Corporation, *OriginPro, Version 2022*, Northampton, MA, USA.
[60] R. K. Harris, E. D. Becker, S. M. Cabral de Menezes, P. Granger, R. E. Hoffman, K. W. Zilm, *Pure Appl. Chem.* **2008**, *80*, 59.
[61] Adept Scientific, *gNMR V 5.0*, **2005**.
[62] G. M. Sheldrick, *Acta Crystallogr. Sect. A* **2015**, *71*, 3.
[63] G. M. Sheldrick, *Acta Crystallogr. Sect. C* **2015**, *71*, 3.
[64] O. V. Dolomanov, L. J. Bourhis, R. J. Gildea, J. A. K. Howard, H. Puschmann, *J. Appl. Crystallogr.* **2009**, *42*, 339.
[65] A. D. Becke, *J. Chem. Phys.* **1993**, *98*, 5648.
[66] M. Sierka, A. Hogekamp, R. Ahlrichs, *J. Chem. Phys.* **2003**, *118*, 9136.
[67] S. Grimme, J. Antony, S. Ehrlich, H. Krieg, *J. Chem. Phys.* **2010**, *132*, 154104.
[68] a) F. Weigend, R. Ahlrichs, *Phys. Chem. Chem. Phys.* **2005**, *7*, 3297; b) F. Weigend, M. Häser, H. Patzelt, R. Ahlrichs, *Chem. Phys. Lett.* **1998**, *294*, 143.
[69] A. Schäfer, H. Horn, R. Ahlrichs, *J. Chem. Phys.* **1992**, *97*, 2571.
[70] TURBOMOLE GmbH, *TURBOMOLE V7.3. development of University of Karlsruhe and Forschungszentrum Karlsruhe*, **2018**.

Manuscript received: November 22, 2022
Accepted manuscript online: January 4, 2023
Version of record online: March 3, 2023